FR9401673

I.P.N. - 91406 ORSAY CEDEX

institut de physique nucléaire CNRS - IN2P3 UNIVERSITÉ PARIS - SUD

IPNO-DRE. 93-14

MESON PRODUCTION FROM N-N COLLISIONS

N. WILLIS
Institut de Physique Nucléaire,
BP n° 1 - 91406 Orsay France

IPNO-DRE. 93-14

MESON PRODUCTION FROM N-N COLLISIONS

N. WILLIS
Institut de Physique Nucléaire,
BP n° 1 - 91406 Orsay France

Invited talk to the workshop on Meson production in Nuclear collisions
GSI - Darmstadt, May 5th, 1993

SUMMARY

MESON PRODUCTION FROM NN COLLISIONS

N.Willis

I.P.N. BP N°1, Orsay, 91406 France

Light meson production as π,η.. have been extensively explored recently in many laboratories, at intermediate energies(0.3 to 2.5 GeV). First, the expansion of the experimental informations available in the pion production field, including now spin observables, was facilitated by the developpments of intense polarized beams and polarized targets. The progress on experimental technics of detection allowed complete measurements of the three-body final state reactions which are known to constitute the bulk of inelasticities in this energy range. The importance of the Δ^{++} role have been pointed out many years ago in total and differential cross-sections analysis mainly for the pp$\rightarrow$ pnπ^+ reaction. Recent sophisticated calculations trying to account for the different channels(NN $\rightarrow$ NN, NN$\rightarrow$ Dπ^+, NN $\rightarrow$ NNπ..) in an unified way have shown that others N^* resonances should play an important role especially to understand spin observables. This leads experimentalists to explore others inelastic channels as NN $\rightarrow$ NNη where N* appears to dominate (maily S^{11}1535 MeV and P^{11}1710 MeV). The important cross-section near threshold makes this experiment highly feasible at Saturne National laboratory. This is mainly due to the vicinity of the S^{11} and to a strong ηN interaction.

In a first part recent experimental results on pion production in different channels leading to a 3-body final state (pp$\rightarrow$pnπ^+, pp$\rightarrow$ppπ^o, np$\rightarrow$ppπ^-) are reviewed. In a second part new data in the η production channel are presented.

In the two cases results are compared to calculations either in a coupled channel calculation or in a first order pertubative approach. The role of NΔ and NN* mechanisms are pointed out.

I - INTRODUCTION

Meson production in nucleon-nucleon collisions is really a too large field to be explored in a limited time. It seems reasonable to concentrate my talk in the intermediate energy range (0.3 → 2.3 GeV) on light meson production (π, η, η') where the importance of nucleon resonances (Δ^{++}, Δ^{+}, N*) have been pointed out. This means, I will skip all the strangeness production through K production. In the π production, I will skip completely the study of the pp → dπ^+ reaction which would have required all the time of this talk: so many experimental results have been obtained for a long time. In fact this reaction has been studied almost as completely as the NN elastic channel, including spin observables in the two reverse $\vec{p}\,\vec{p} \rightarrow d\pi^+$ and $\pi^+ d \rightarrow$ pp channels. From an experimental point of view this is of course due to the fact that it is a 2 body reaction. Even if the vigorous experimental program have initiated also a theoretical effort, the 3 body channel NN → NNπ is the dominating inelastic channel of nucleon-nucleon scattering and a tremendous amount of experimental data and theoretical calculations have been obtained these last years. Last developments of calculations have shown that beside the well know importance of the Δ(33) resonance, others N^* resonances should be taken into account, especially to understand spin observables. This leads experimentalists to explore inelastic channels as NN → NNη around the kinematical threshold where the S^{11} (1535 MeV) resonance appears to dominate.

So I will divide my talk in a first part centred around last results of meson production experiments through the Δ mechanism then in another part on meson production through NN^* mechanism.

II - NN → NNπ

Study of π production has now a long history for several reasons :

- The πNN system is important because of the π exchange nature of the strong interaction and it is a fundamental testing ground in the effort to build a consistent theory of the nucleus taking into account the π, Δ, N* degrees of freedom.

- The first studies in the 60's and 70's were also strongly related to the structures found in pp ($\Delta\sigma_L$) elastic scattering [1] in the GeV range. The driving force of the experimental and theoretical effort was the possibility that the NN interaction may involve exotic dibaryonic resonances, objects that might be associated with quark and colour degrees of freedom. Those "dibaryons" candidates were thought to be strongly coupled with the πNN channel and their effects should be seen in one pion production channel. In the considered region the opening of the N-Δ channel could also explain resonance-like behaviour in some partial waves as the NN $^1D_2$ and $^3F_3$ waves.

In order to know if the data require a quark explanation it was necessary to develop a conventional approach as complete as possible.

Paralleling this progress, experimental new programs were necessary to test carefully the calculations, especially to study spin observables which are known to be sensitive to the details of the interaction mechanism and also to study the energy dependence of eventual structures that might be associated with resonances.

- Finally, we have to remember that in the intermediate energy range NN $\rightarrow$ NNπ constitute the bulk of inelasticities of the NN system : for example at 800 MeV (pp) total cross section ($\simeq$46 mb) is nearly equally divided between the elastic ($\simeq$25 mb) and single pion production channels ($\simeq$21 mb).

This explains the reasons of the renewal of this field in the last 10 years with mainly :
- the improvement of theoretical calculations trying to describe in a consistent way

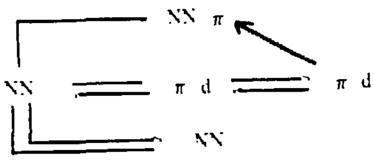

- the expansion of the experimental informations available on the one single pion production process. This was facilitated by the development of intense polarized beams and polarized targets now available. The progress on experimental technics of detection allowed measurements of so called "exclusive" reaction studies, i.e. when the 3-body final state was completely determined.

1. General considerations

a) Early stage of NNπ physics

i) Measurements :

Extensive investigation of integrated cross sections at various energies for different channels have been performed in different laboratories :

$\sigma(pp \rightarrow \pi^+ pn)$	see compilations by Bystricky et al. [2]
$\sigma(pp \rightarrow \pi^\circ pp)$	for LAMPF, TRIUMPF, SATURNE results
$\sigma(pn \rightarrow \pi^+ nn)$	
$\sigma(pn \rightarrow \pi^+ nn)$	Shimizu [3] for KEK results.
$\sigma(pn \rightarrow \pi^- pp)$	
$\sigma(pn \rightarrow \pi^\circ pn)$	

ii) At 800 MeV the (pnπ^+) cross section is found to be the most important ($\simeq$ 18 mb) compared to (ppπ°) channel ($\simeq$ 3-4 mb) and pp $\rightarrow$ dπ^+ channel ($\simeq$ 1.5 mb).

iii) Most of the models are OPE peripheral models and showed the Δ^{++} dominance (at 500 MeV, 75% of the ($pn\pi^+$) cross-sections proceeds though Δ^{++} resonance). They failed in reproducing at the same time π^+ and π° cross sections as shown in the fig.1. The π^+ cross section is overestimated by a factor of 2 above 600 MeV and the π° cross section slope and values are not reproduced. This trouble subsists when one introduces a vertex form factor with increased cut off masses and is related by different authors to the lack of the spin triplet inelastic strength already seen in NN $\rightarrow$ NN and NN $\rightarrow$ πd reactions.

iv) Silbar and Kloet[4)] in the 80's presented first results of a calculation of total, elastic and inelastic single π production cross-sections in a unitary relativistic three body model (fig. 2). In this conventional model the contribution of $^1D_2$ and $^3F_3$ partial waves were found to have a resonance like-behaviour due to the strong N-Δ coupling in both elastic and inelastic cross-sections. Very large spin effects are seen for both elastic and inelastic channels and new measurements were really needed.

v) There are a few experiments in the np channels[5]. The experiments were done using either deuterons as neutron targets or neutrons beams from stripping reactions. The quality of the results were not very good and used mainly to deduce the cross section in the I = 0 entrance channel $\sigma_0 = [2\sigma(np \rightarrow \pi^+ nn) - \sigma(pp \rightarrow \pi^\circ pp)]$. The controversy of the different results, due to the lack of precision of both experiments is still remaining : I will speak of this when I will discuss new results in these channels (sect. 2).

b. <u>New trends</u>

i) In the experimental field high quality polarized beams and polarized targets become available at LAMPF, PSI, TRIUMF, LNS (Saturne) and KEK allowing spin observables measurements; at least 2 particles are detected over a wide range of solid angles and large space phase is covered.

The important experimental program is matched by a corresponding theoretical effort. The very numerous calculations are based on two main approaches :

- The pion exchange peripheral models as developed by VerWest et al.[6)] et recently by J.M. Laget [7)]or F. Wellers[8].

In the case of Born approximation, the interest is to separate the effect of the different main contributions on the various experimental observables.

In the first order of a diagrammatic expansion of the amplitude, π and ρ exchange are considered in calculations from F. Wellers. Phenomenological final state and initial state interactions are introduced. The P_{33} channel corresponds to a Δ^{++} excitation and others (SPDF) πN waves are included. The cut off masses of the vertex function are determined using deuterium photodesintegration results. In the last calculations corrections with high order terms are introduced.

- In the coupled channel model (CCM) approach[9-10] a set of coupled channels equations driven by the OPE are resolved. Dominant interactions are the P_{33} and P_{11} πN two body interactions. The two body sub-system are assumed to interact through separable

potentials. The two body interactions are defined in a relativistic framework through the vertex functions in terms of relativistic momenta. All P and S π-N waves are taken into account with form factors adapted to fit phase shifts and scattering lengths for P_{13}, P_{31}, S_{11} and S_{31} channels. For the P_{33} waves the parameters of the form factors are constrained by the position of the Δ resonance and the (πN) P_{33} scattering data.
The P_{11} wave is the sum of two contributions ["pole" + "non resonant"].

Various prescriptions are taken to take into account the off shell nature of P_{11} and P_{33} interactions (a new monopole form factor is introduced for example[12]).

There are new improvements of CCM :

- Short range forces are introduced[13] (ω, ρ, σ exchanges) with new form factor at each meson-nucleon vertex. They are chosen to reproduce correctly $^1D_2$ phase shift and inelasticity (fig. 3).

2). pp → pnπ+ channel

At LAMPF, analyzing powers and polarized cross-sections have been measured at 800 MeV incident energy for 12 different proton-pion pairs over a large range of proton momenta by Hancock et al.[14] The data are presented on fig. 4 for different geometrical configurations and compared to predictions from a Fadeev calculation from Garcilazo[15]. It is clear in the experimental cross-section data that this reaction proceeds mainly through pp → Δ^{++}n channel. In the region of the Δ^{++} bump the values of the cross-sections are about one order of magnitude larger at 0° that at 90°. this is in favour of a peripheral reaction.

The data also shows a large contribution from the (n p) final state interaction, with a prominent peak in geometries where the two outgoing nucleons share very small relative momentum. The asymmetry A_{no} clearly increases monotonically towards the value of the proton momentum corresponding to the Δ peak.

Concerning the differential cross-sections the models do rather well and models differences in prediction is rather small, the Born approximation over-predicted the cross section by 20%. (fig 6)

The model predictions are not so good for asymmetries as for the cross-sections. They follow the general trends of the data but give a slope less steep or are below the data.

On fig. 5, a calculation for A_{N0} from F. Sammarucco et al.[16] shows clearly a good agreement at low momenta but fails to reproduce the data at high momenta.

A careful study of the importance of different factors as the contribution of different partial waves and short range contribution leads the authors to conclude that sufficient inelasticities in $^1D_2$, $^3F_3$ channels guarantees a reasonable prediction of cross-sections. On the contrary A_{N0} seems to be controlled by an interplay of spin states and not dominated by a particular partial waves.

The comparison of an impulse and full calculation, the FSI effect, the influence of $^1D_2$ and $^3F_3$ partial waves which are known to be the most important are clearly seen on fig. 6.

Always at LAMPF, the first measurements of spin-spin correlation were performed by Bhatia et al.[17] They measured A_{NN} and A_{LL} at 650 MeV and 800 MeV for a couple of angle pairs and one momentum for the outgoing proton.

The spin correlation parameters A_{SS}, A_{NN}, A_{LL} A_{SL}, and the asymmetries for $pp \rightarrow (p\pi^+n)$ reactions were measured at 420 MeV, 465 MeV and 510 MeV by Shypit et al., then Waltham et al.[18] at TRIUMF and the measurements were extended to higher energies by Shypit et al.[19] (492 → 786 MeV) at LAMPF. The results are presented on fig. 7 together with CCM calculations from Dubach et al. The agreement is not really fair and the origin of the discrepancy was not really found.

Hollas et al.[20] performed the first measurements of spin transfer coefficients at 800 MeV. The trend of the data appears to be qualitatively reproduced by the model from Ueda[9] (fig. 8).

Dubach[21] has carefully studied the ingredients of a similar calculation on these data and concluded that spin observables are not very sensitive to short range part of the interaction. The most important partial waves are always $^3F_3$ and $^1D_2$ but the details of spin observables are due to the remaining partial waves.

A very extensive data set from an earlier experiment at Argonne has been published by Wicklund et al.[22] The data were taken over a large phase space. Differential cross-sections and analyzing powers were deduced for $NN \rightarrow N\Delta$ reaction from which a partial wave analysis was performed and the corresponding scattering amplitudes were determined. This is important for the questions of the nature of the structures observed in NN $^1D_2$ and $^3F_3$ channels. If they are resonances the amplitudes to $^5S_2$ and $^5P_3$ N-Δ states should vary rapidly with energy. They found a slow variation of theses amplitudes and this argued in favour of a classical threshold effect in these channels.

The $\delta_{N\Delta}$ phase for $^1D_2 \rightarrow {}^5S_2$ channel has been extracted and is presented on fig. 9. This phase is very large (60°) around the NΔ threshold and decreases around $T_p \simeq$ 800 MeV to 11°. This indicates a possible attractive N-Δ interaction in this channel.

On another side the Argonne data have been recently compared to a three body calculation. One can see on fig. 10 that the agreement is acceptable for the integrated differential cross-section $d\sigma/d\cos\theta_\Delta$ (mb). Concerning the asymmetry the description is correct at 0.57 GeV but is still in disagreement with the data at others energies. The deficiency of the model to reproduce the spin correlation parameters $P_{y\rho_{33}}$ is found to be associated with the lack of strength of the interaction in the $^3F_3$ channel.

An experiment has been carried at Saturne to study the reactions $pp \rightarrow n\Delta^{++}$ and $pp \rightarrow \Delta^\circ\Delta^{++}$.
On the SPES3 beam line at 1.5 GeV and 1.8 GeV incident energy. At the present time the data are under analysis (fig. 11).

3. Study of $pp \rightarrow pp\pi^\circ$ channel

In terms of the isospin of the nucleons pair involved respectively in the entrance and exit channel, the cross section of this reaction can be expressed as

$$\sigma(pp \rightarrow pp\pi_o) = \sigma_{11}$$

and the reaction $np \rightarrow pp\pi^-$ as $\sigma(np \rightarrow pp\pi^-) = 1/2\,(\sigma_{01} + \sigma_{11})$.

So the measurements of these two channels are important in order to extract σ_{01} cross section which is not well known and probably very small below 1 GeV.

The σ_{01} cross section cannot proceed through ΔN intermediate state and so one can expect that some others mechanisms such as NN* intermediate states will be seen, not being hidden by the strong NΔ interaction. In the case of pp → ppπ° reaction this channel is dominated by Δ^+ which is ten times less strong than Δ^{++}.

There are three recent experiments in this channel :

- The data from Ryley et al.[23] at LAMPF measuring the induced proton polarisation P_Ω and spin transfer coefficients D_{NN}, D_{SL}, D_{LL} at 800 MeV, 733 MeV and 647 MeV are presented on fig. 12. The set-up was the same as for Hollas (pπ^+n) measurements. The calculation from Dubach et al. shows clearly the Δ^+ contribution. The agreement with the data concerning the spin observables, is found to be not so fair than for (pπ^+n) reaction.

In the case of pp → ppπ° there are several contributions of comparable weights and the role of the P_{11} interaction in the Δ^+ or N* should be emphasized.

I will skip on the others measurements at threshold from Stanislaus et al.[24] to come to an experiment performed at Saturne using SPES0 spectrometer (fig. 13). Didelez et al.[25] have measured total, differential cross-sections and analyzing powers for pp → ppπ° from 325 MeV to 1012 MeV incident energies. The two γs rays from the π° decay were detected in lead glass barrels. Using (np) → (nnπ^+) previous results, σ_{01} cross sections were extracted. The calculation, from Laget reproduces quite well the results below 700 MeV.

The predicted asymmetries are positive with a maximum value around 120° even th ough the measured values are negative (fig. 14).

4. np → ppπ^- measurements

As for pp → ppπ° reaction Δ^{++} intermediate state is forbidden. In the I = 0 channel the Δ contribution is completely forbidden whereas in the I = 1 channel the Δ° contribution is weak. So the contribution of the I = 0 channel should be seen in exclusive experiments and spin observables.

In order to study the reaction, the polarized neutron beam available at LNS (Saturne) was used[26]. The reaction products were measured by means of a 4π solid angle detector Arcole at 572, 784, 1022 and 1134 MeV incident energy .

The set up (fig. 15) was designed to measure the 6 angles of the 3 outgoing particles which permits a complete determination of the kinematics and provides an over determination of the reaction. Additional dE/dx and TOF informations were also measured. Angular distributions of asymmetries were measured in 98% of the total phase space.

Strong values of analyzing powers Ay were observed. Calculations are from Laget and π, ρ exchange are taken into account . Partial waves are included up to F; the P_{33} wave is described by the Δ isobar model. As can be seen on fig. 15, the trend of the data is missed especially at backward angles. This peripheral model which accounts generally for the main features of the cross sections might be not enough sophisticated to describe spin observables.

III - NN → NNη and the NN+ interaction.

The most noticeable difference between the π^o and η is the isopin 1 for π^o and 0 for η meson ; this makes impossible for the η to be coupled to the Δ resonance whereas the π^o couples with both Δ and N*. This selectivity as regard to resonances has been seen in the highly structured excitation function of the pd → 3Heη and pd → ^{3}Heπ^o on figure 16.The large value of the cross section near threshold and the bumps in the excitation function for the η production correspond to the excitation of the $N^*(1/21/2)$ resonances. In the vicinity of the η threshold the S_{11}(1535 MeV) resonance has a strong S coupling to Nη (45 to 55% decay in the Nη mode), and gives rise to very sharp energy behaviour for η production and correspond to a dip in π^o production. The importance of the cross sections values near threshold makes experiments highly feasible in the pp → ppη channel and this induces also several calculations based mainly until now on pertubative approaches.
The cross-sections corresponding to the following diagram have been estimated by three different groups.

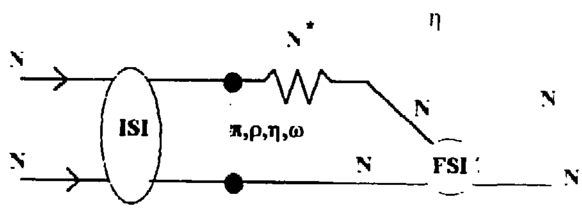

In all cases the η's come from the decay of N* resonances wich are produced by the exchange of various mesons.

a) J.F. Germond and C. Wilkin[27] introduced only N* (1535 MeV) and therefore their calculation is only valid near threshold. The π and η couplings to the N* are deduced from the decay width of this resonance. The ρ and ω coupling are deduced from the photo production data γp → N*. Initial and final state interactions are taken into account.

b) J.M. Laget, F. Wellers and Lecolley[28] included form factors at the vertices instead of initial state distorsion. Other partial waves, in addition to the N* (1535 MeV), have been included; this is important when incident energy increases.

c) Vetter et al.[29] kept only S wave ηN interactions and determined the ρ coupling from the small $\pi\pi$ tail of the ρ. They neglected both ISI and FSI.
The two first groups agree that ρ exchange contribution is more important (by factor 5 → 10) than the π exchange one. The third group don't find as big an effect. The two first models are also applied to np → dη channel near theshold as it will be seen.

1. pp → ppη clannel.
The crucial lack of data near threshold led us to perform an experiment[30)] using the SPES3 spectrometer and its experimental set up at Saturne (LNS) (Fig 17).

In this experiment, the two protons were detected by means of wire chambers and the missing mass was calculated. At a nominal field of 3.1 Teslas the spectrometer has a rather wide momentum acceptance (600 to 1400 MeV/c) with a mean angular acceptance of 10^{-2} sr. This is well adapted to the measurement of total η production cross-section in the vicinity of the threshold in one measurement at 0°. The correlation between the momenta of the two detected protons is seen on figure 17.a. The blank region along the diagonal is due to tthe lack of efficiency in the case where the 2 protons hit the same detector. The corresponding kinematics for pp → ppπ°, pp → pp+2π and pp → ppη are presented on figure 17.b.

Proton beams of 1260, 1265 and 1300 MeV were incident on a cryogenic H_2 target. The data and results of the calculations quoted above are presented on figure 18.

It is clear that the total cross section shows a pronounced energy dependance which might indicate a resonant effect near threshold. The existing models with the different assumptions quoted in the figure caption fail to reproduce the data.

The experimental technics used on SPES3 beam line is only valid near threshold as the two protons angle increased rapidly with incident energy. At higher energies the detection of the η decay products to identify the η particle is more convenient. This has been performed at Saturne by the PINOT collaboration[31)]. Their spectrometer figure 19a. was constructed to detect the 2 γ rays issued from η decay at energies between threshold and 1700 MeV . The data are not yet published but the results at the lowest energies are in good agreement with ours.

2. np → dη and np → npη reactions

Until recently no data exist on η production in the np channel. Two surprises came from :

i) The experiment on PINOT beam line : this group measured the η production with a proton beam on an H_2 an a D_2 liquid targets with the same configuration of the spectrometer. The differential cross section ratio for the kinematical conditions $0° \leq \theta_{\eta}^{lab} \leq 14°$ are shown on figure 19b for Tp = 1300 MeV and Tp = 1500 MeV.

At Tp = 1300 MeV, the contribution of np → dη process is probably important and this might explain the difference between the ratios at the two energies. The kinematical cut is more stringent for the pd reaction than for the pp reaction due to the different phase space covered and the Fermi momentum in the deuteron. Taking into account those effects, the authors concluded to a ratio about 8 between pn → pnη and pp → ppη reactions which is not theoretically understood at the present time.

ii) A reanalysis[32)] of old np → dX data[33)] : this experiment was done at Saturne with a 1.88GeV/c neutron beam obtained by stripping a 3.76 GeV/c deuteron beam on a beryllium target. The central neutron energy was below the η threshold but 10% of the neutrons had an energy above the threshold to the Fermi momentum spread in the primary deuterons. The authors have performed Monte-Carlo calculations for 1π, 2π, 3π...contributions in order to extract np → dη reaction. They extracted a value of σ_{η} = 110

± 15 μb, a few MeV above threshold. This result is quoted on figure 20 together with J.M. Laget et al.[28]. New experimental results are obviously needed in this region !

Others channels as pd → $^3He\eta$, $\pi^- p \rightarrow \eta n$ etc... channels are actually also studied. It is out of this talk to discuss all these results but intensive calculations are also done in order to analyse and understand the basic mechanism.

CONCLUSION

In the pion production section :

The reaction pp $\rightarrow$ pnπ^+ has been strongly studied experimentally and theoretically. The data on spin observables are not sufficient in others channels (in particular in np channels). Models do rather well for cross sections and fail for spin observables. Heavy meson exchange goes in the right direction but is still not sufficient to explain data.

In the case of η, η' ω production, data are still needed in the intermediate energy range in order to valid calculations.

Aknowledgments :

I would like to thank GSI Darmstadt organizers to give me the opportunity to present new results in this field. I thank also J.P. Didelez and E. Vercellin who communicated respectively the results of the Orsay-Bonn-Columbia collaboration and the Torino collaboration prior to publication.

REFERENCES

[1] A. YOKOSAWA, Proc. 19th Int. Conf. on high Energy Physics, Tokyo, 1978, p. 121 ; I.P. AUER, Nucl. Phys.A335 (1980) 193

[2] J. BYSTRICKY et al., J. Phys. 48 (1987) 1901

[3] F. SHIMIZU et al., Nucl. Phys. A386 (1982) 571

[4] J. KLOET and R. SILBAR, Nucl. Phys. A338 (1980) 281 ; A426 (1984) 625

[5] T. TSUBOYAMA et al., Nucl. Phys. A486 (1988) 669
L. DAKHNO et al., Phys. Lett. 114B (1982) 409

[6] B. VERWEST et al., Phys. Rev. C25 (1982) 1979

[7] J.M. LAGET et al., Phys. Lett. B257 (1991) 254 and ref. therein

[8] F. WELLERS in Proc. 4th Intern. Symp. on Mesons and Nuclei Czech. J. Phys. B39 (1989) 72 and references therein

[9] T. UEDA, Prog. Theor. Phys. 76 (1986) 729
id. page 959

[10] H. GARCILAZO and T. MIZUTANI "πNN Systems World Scientific Press (Singapour 1990)" and ref. therein

[11] BORIE et al., Z. Physik 267 (1974) 393

[12] G. LAMOT et al., Phys. Rev. C35 (1987) 239

[13] T. MIZUTANI et al., Phys. Rev. C47 (1993) 56

[14] A. HANCOCK et al., Phys. Rev. C27 (1983) 2742

[15] H. GARCILAZO and T. MIZUTANI, Few Body syst. 5 (1988) 127 and

[16] F. SAMARRUCA and T. MIZUTANI, Phys. Rev. C41 (1990) 2286

[17] T. BHATIA et al., Phys. Rev. C28 (1983) 2071

[18] C. WALTHAM et al., Nucl. Phys. A433 (1985) 649

[19] R.L. SHYPIT et al., Phys. Rev. C40 (1989) 2203
Phys. Rev. Lett. 60 (1988) 901
Phys. Lett. 124B (1983) 314

1400

[20] C. HOLLAS et al., Phys. Rev. Lett. 55 (1985) 29

[21] J. DUBACH et al., Nucl. Phys. A466 (1987) 573

[22] A. WICKLUND et al., Phys. Rev. D35 (1987) 2670

[23] PJ. RILEY et al., Phys. Lett. B197 (1987) 23

[24] S. STANISLAUS et al., Phys. Rev. C44 (1991) 2287

[25] J.P. DIDELEZ
Private communication for the Orsay-Bonn-Columbia collaboration.

[26] Y. TERRIEN et al., Phys. Lett. B294 (1992) 40

[27] J.F. GERMOND and C. WILKIN, Nucl. Phys. A518 (1990) 308

[28] J.M. LAGET, F. WELLERS and J.F. LECOLLEY, Phys. Lett. B257 (1991) 254

[29] T. VETTER et al., Phys. Lett. B263 (1991) 153

[30] A.M. BERGDOLT et al., SPES3, Collaboration - To be published -

[31] C. DELLACASA (private communication) and to be published
E. CHIAVASSA et al., Proceedings of 6ème Journée d'Etude Saturne -
Mont St Odile (1992)

[32] F. PLOUIN et al., Phys. Rev. Lett. 65 (1990) 690

[33] F. PLOUIN et al., Nucl. Phys. A302, 413 (1978)

FIGURE CAPTIONS

Fig. 1 : a) Total pion cross-sections as function of lab. energy calculated by Borie et al.[11] in an OBE model. The pion goes through the Δ (P33) pole and the nucleon P_{11} pole (dashed curves).
b) Same for the pp → pnπ^+ and pp → ppπ^o channels in a Deck model with full πN scattering amplitude as input.

Fig. 2.: Total elastic and inelastic NN → NNπ cross-sections for various channels versus incident proton energy from ref. 4.

Fig. 3 : Phase shift and inelasticity parameters for $^1D_2$ and $^3F_3$ with short range contributions (solid line) and without (dashed line). Data are from Arndt and calculations from 16).

Fig. 4 : Differential cross-sections and A_{NO} in a CCM model[15]. Data in the lab. system are from Hancock at al. [14] at 800 MeV. Given are the lab. proton and pion angles and the CM Δ^{++} production angle.

Fig. 5 : CCM calculation of A_{NO} by Sammarucca et al. [16] for pp → pnπ^+ reaction at 800 MeV for two different kinematical conditions. Data are from Hancock et al. [14].

Fig. 6 : a) pp → pnπ^+ differential cross section calculated at 800 MeV by Mizutani [13]. Comparison of the full calculation (solid line) with the impulse result (dashed line).
b) Same as in a). The solid curve is a result of the calculation keeping Δ^{++} production. The dashed (dot-dashed) curve corresponds to a calculation including $^3S_1$ - $^3D_1$ ($^3S_1$ - $^3D_1$ and ^1S_o) nucleon-nucleon final state interactions.
c) Effet of omitting a) $^1D_2$ (dashed) or b) $^3F_3$ (dashed) in the calculation.

Fig. 7 : A_{NO}, A_{ON} and A_{SL} measured by Waltham et al. [18]. Solid line are predictions from Dubach [21].

Fig. 8 : Polarisation observables of $\vec{p}$p → $\vec{p}\pi^+$n calculated by Ueda[9] for following (ϕ_p, ϕ_Δ) : (8°, 8°), (15°,40°) and (22°,68°) respectively in a)b)c)d) and for ϕ_π = 95°. The data and dotted curves are from Hollas et al.[20].

Fig. 9 : The phase shift $\delta_{N\Delta}$ extracted by Shypit [19].

Fig. 10 : (a) Integrated cross-sections and (b) production asymmetry A_y for the NN → NΔ reaction at various energies [22].
(c)(d) : integrated spin correlations in the same conditions.
The full calculation from Mizutani et al. [13] is given with (solid line) and without the ρ exchange contribution (dashed line).

Fig. 11 : Experimental spectra for $pp \rightarrow pn\pi^+$ reactions at T_p = 1500 MeV and 1800 MeV. Correlations between the momenta for the detected pion and proton are seen for the missing masses corresponding to a neutron or a Δ°.

Fig. 12 : (a) Spin average proton momentum distribution spectrum for $pp \rightarrow pp\pi^\circ$ reaction [23] at 800 MeV. Calculation from Dubach et al. [21] is averaged in the angular experimental acceptance.
(b) Depolarization observable D_{NN} in the same conditions.

Fig. 13 : Comparison of experimental results for $pp \rightarrow pp\pi^\circ$ cross-sections[25] with J.M. Laget calculations.

Fig. 14 : Same as Fig.13 for analyzing power A_y. Stars are for J.M. Laget calculations. Crosses correspond to experimental results[25].

Fig. 15 : a) The vertex detector Arcole. General layout.
b) Angular distributions of the measured analyzing power in the $\vec{n}p \rightarrow pp\pi^-$ reaction at (a) 572 MeV ;
c) 784 MeV ;
d) 1012 MeV (squares) and 1134 MeV (diamonds). The calculation is from Laget [7].
The data are from [26].

Fig. 16 : The $\theta_\pi = \theta_\eta = 180^\circ$ excitation function of $pd \rightarrow {}^3He\pi^\circ$ and $pd \rightarrow {}^3He\eta$ reactions as a function of the total CM energy minus two nucleon masses ref.[34].

Fig. 17 : Calculated (a) and measured (b) correlations between the two detected protons in the reaction $pp \rightarrow ppX$ for T_p = 1265 MeV and T_p = 1300 MeV.

Fig. 18 : Total cross section data near threshold for the $pp \rightarrow pp\eta$ reaction measured on SPES3 beam line[30]. (GW) corresponds to a calculation [27] with a pure ρ exchange. (GWM) corresponds to a complete calculation with [27] prescriptions for the relative phases for π, η and ρ exchange. The curves LWLI and LWLII are those of ref. [28].

Fig. 19 : (a) Pinot γ rays spectrometer : Layout of one arm.
(b) Cross-section ratios for $pd \rightarrow \eta X$ over $pp \rightarrow \eta X$ as measured by PINOT collaboration[31].

Fig. 20 : The total cross-section of the $np \rightarrow d\eta$ reaction versus the incoming neutron laboratory kinetic energy. Calculations from [28] include η direct graph (dotted), π exchange graph (dot-dashed) and $(\pi+\rho)$ exchange (full and dashed) with respectively Λ_ρ = 2.15GeV or Λ_ρ = 2m.

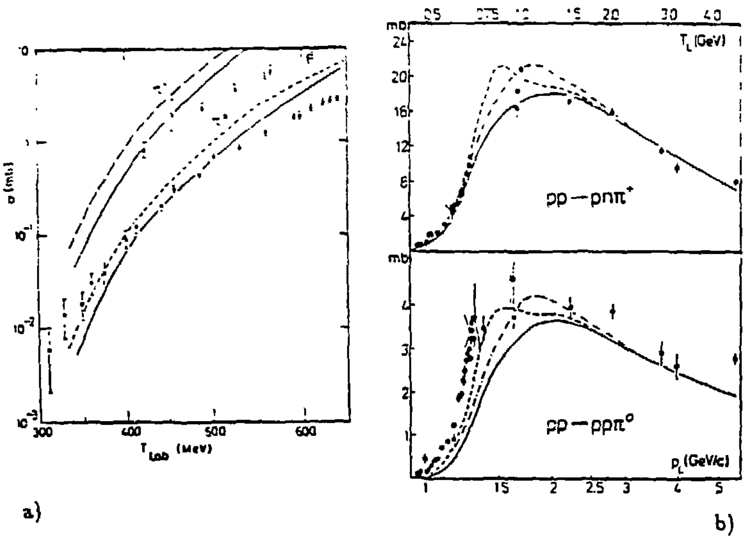

Figure 1

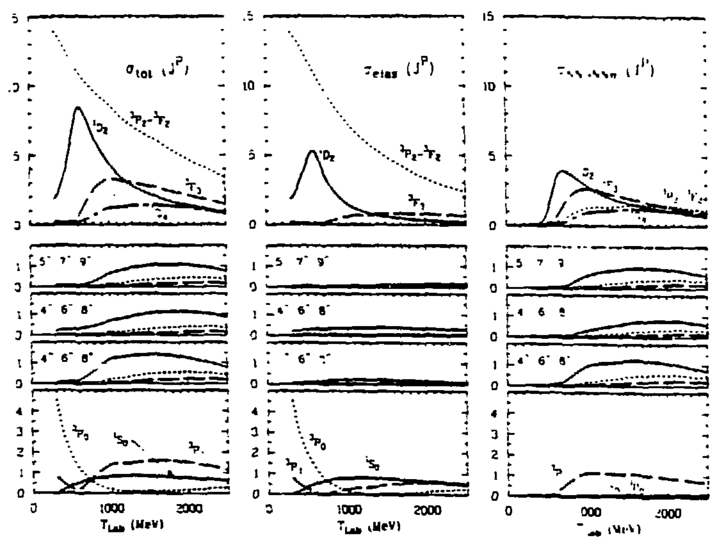

Figure 2

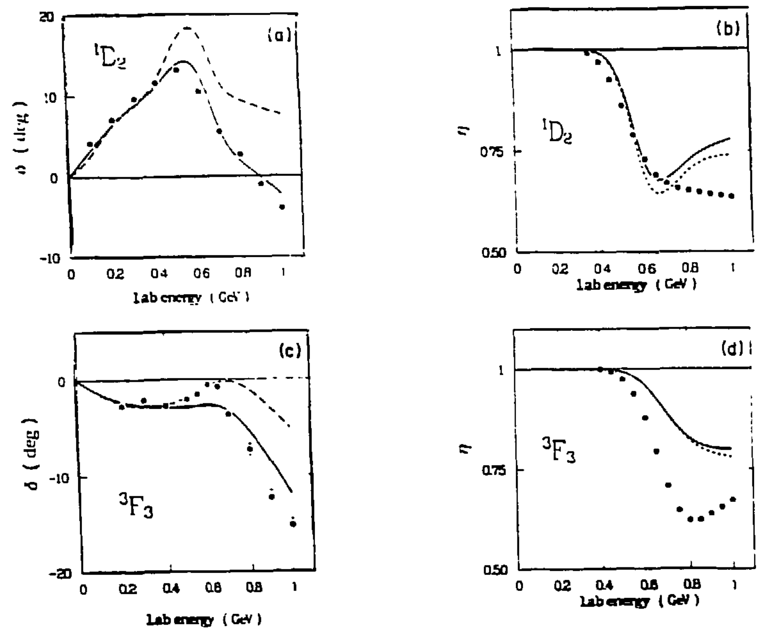

Figure 3

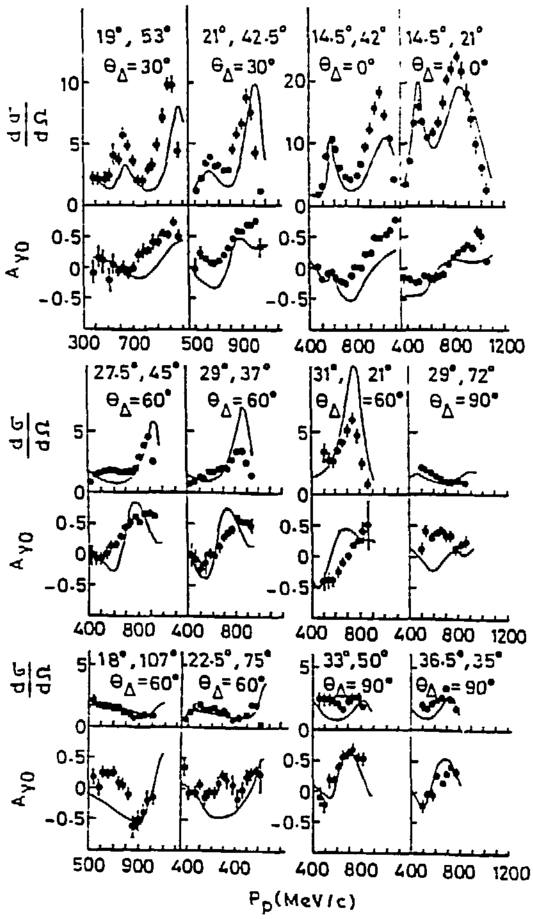

Figure 4

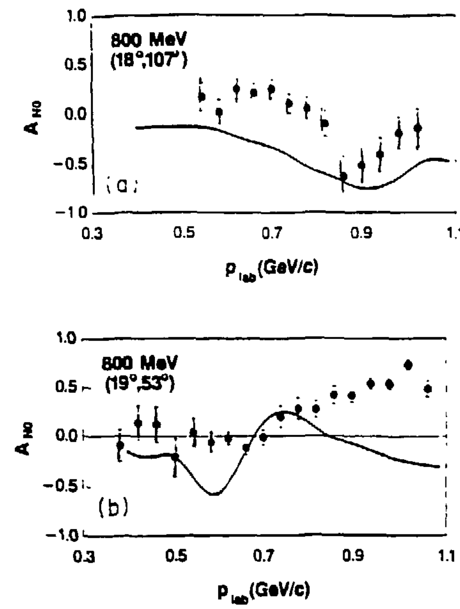

Figure 5

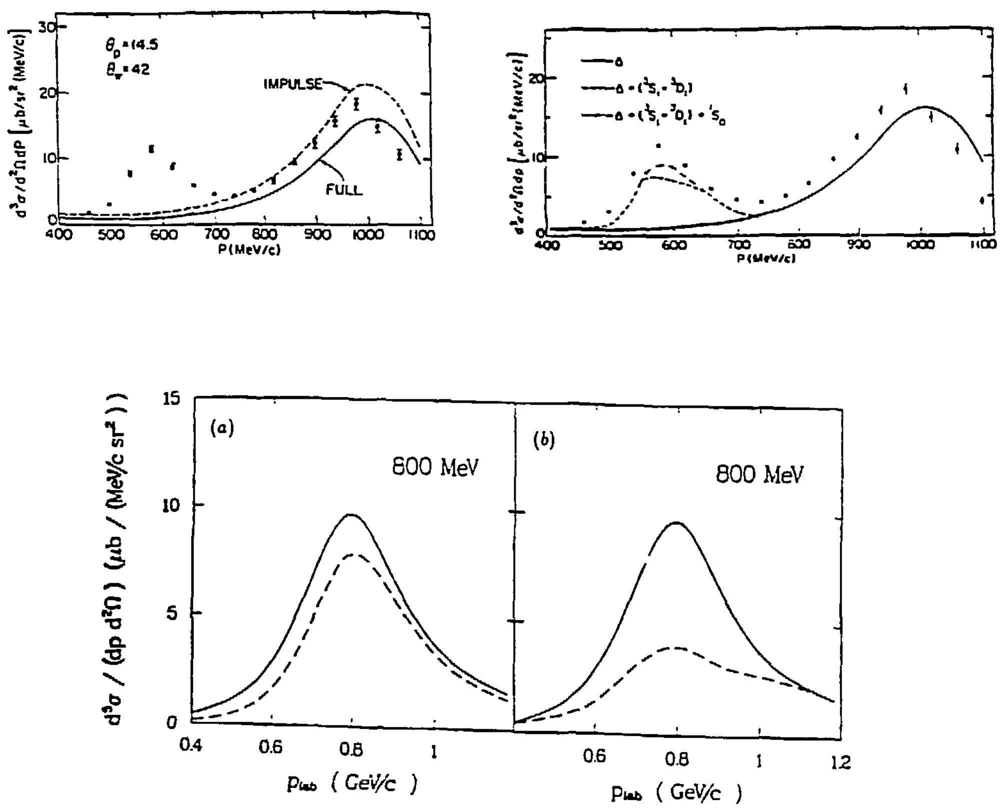

Figure 6

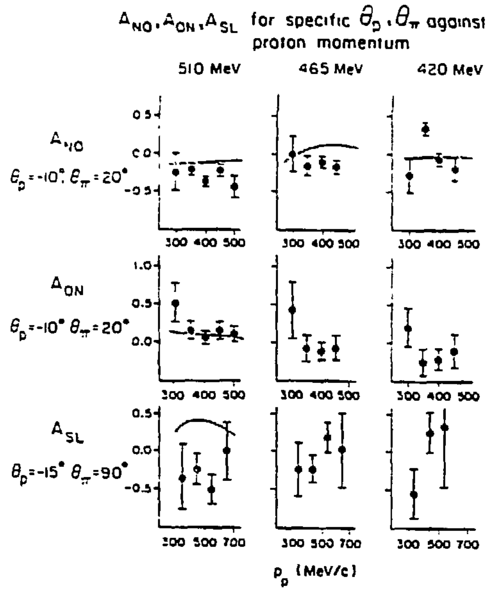

Figure 7

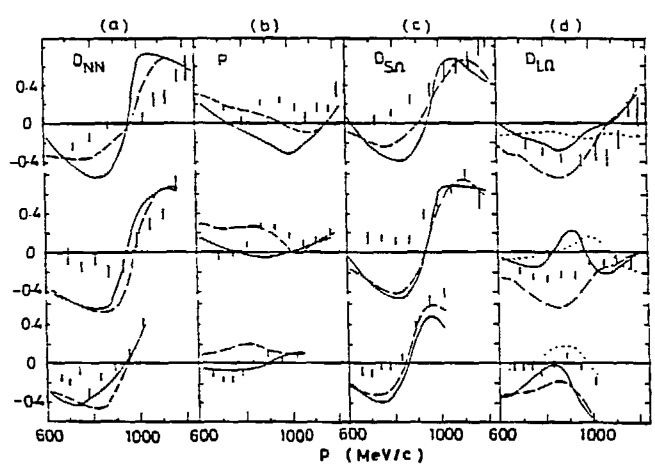

Figure 8

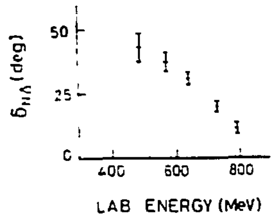

Figure 9

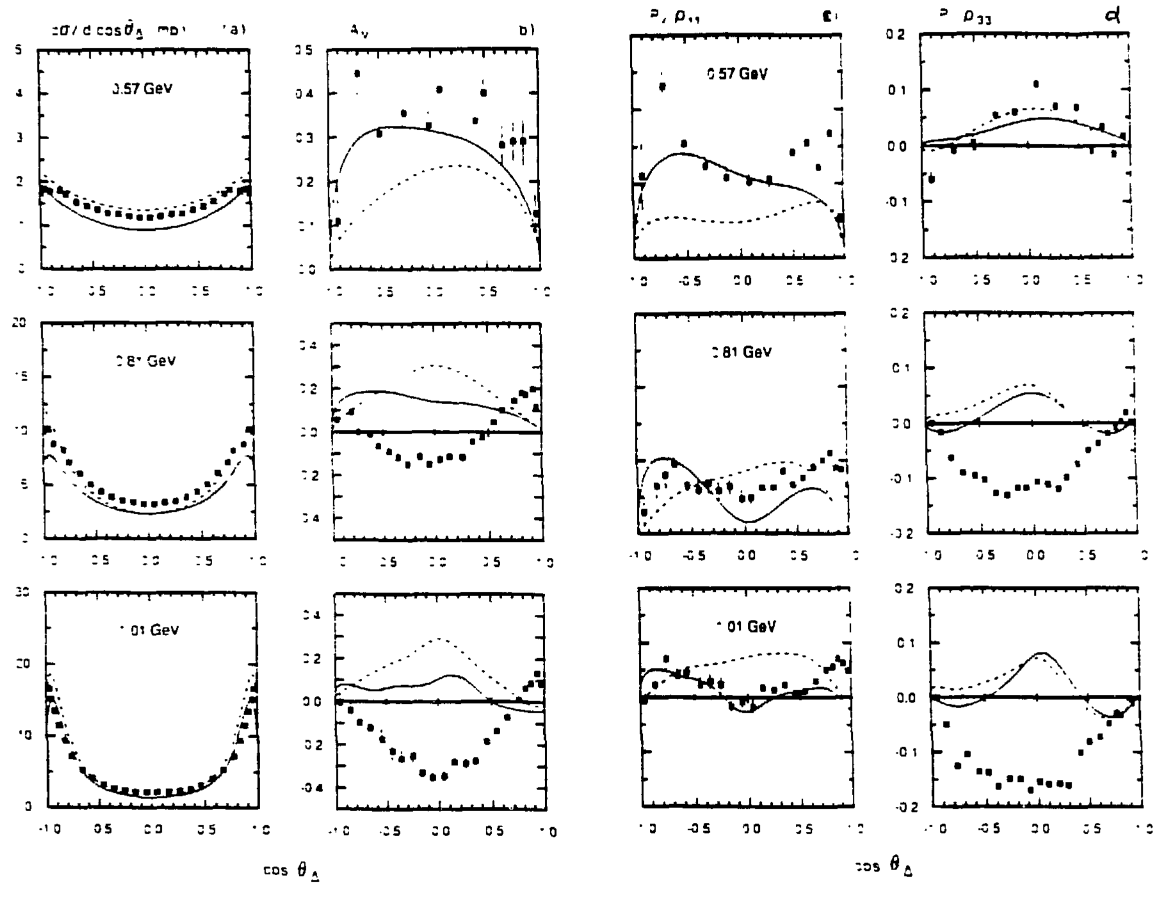

Figure 10

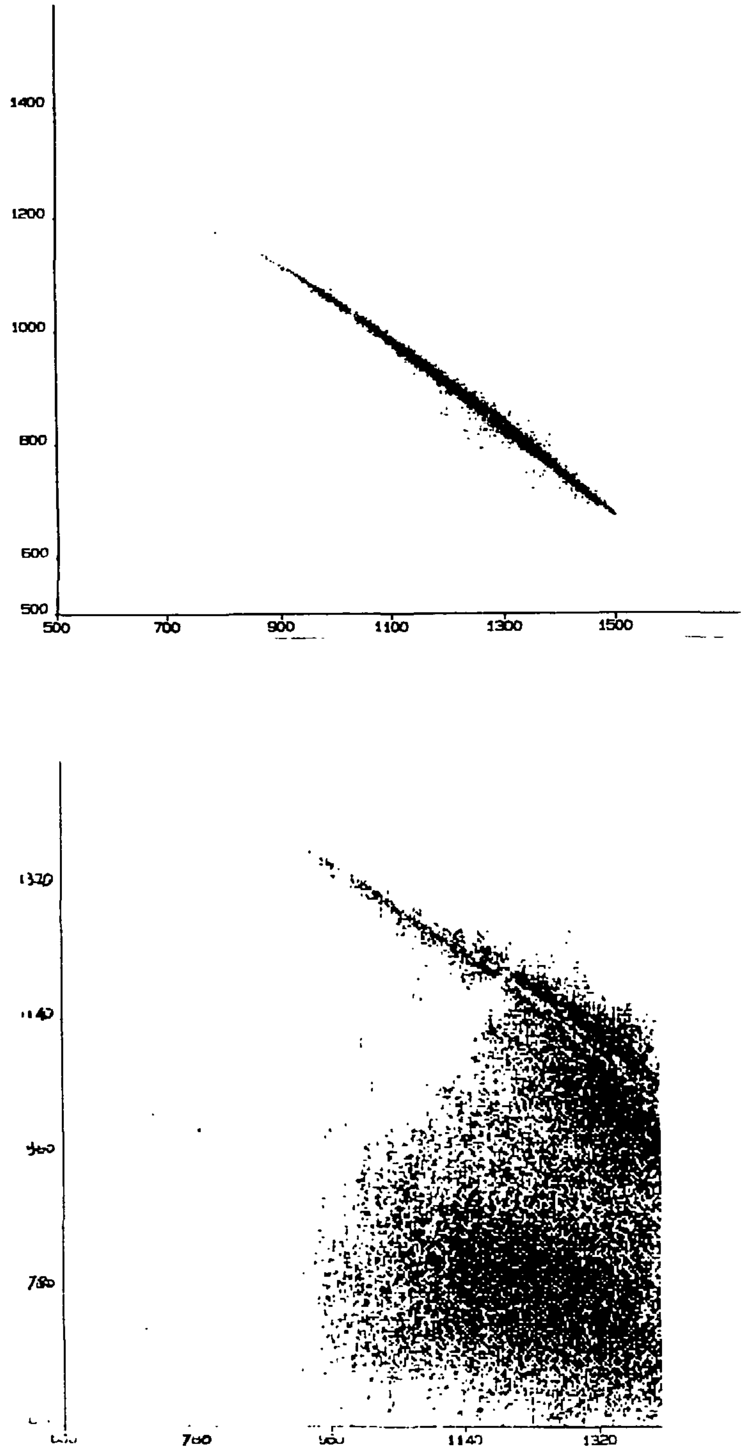
1400
1200
1000
800
600
500
500
700
900
1100
1300
1500
1320
1140
960
780
780
960
1140
1320

Fig. 11

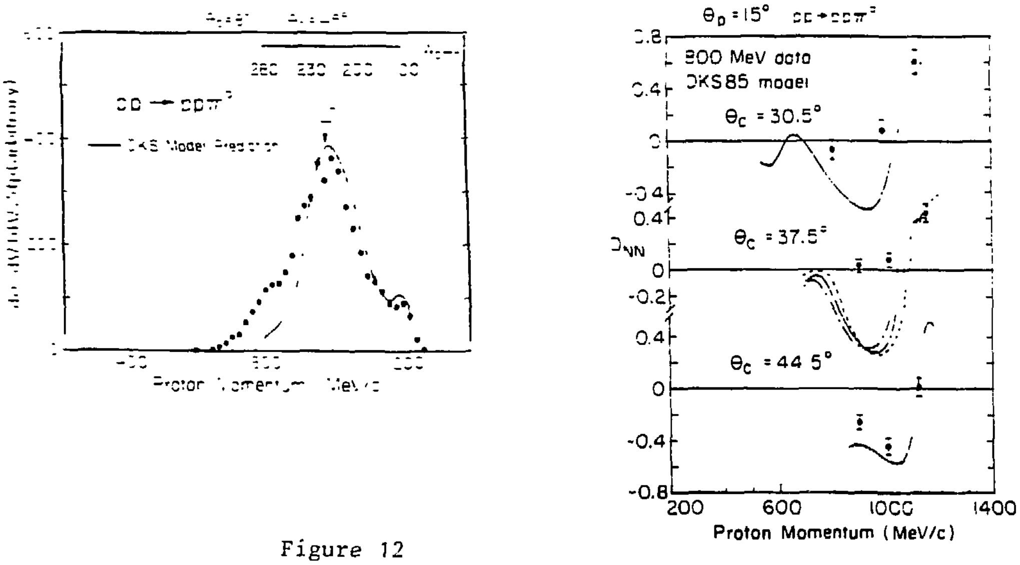

Figure 12

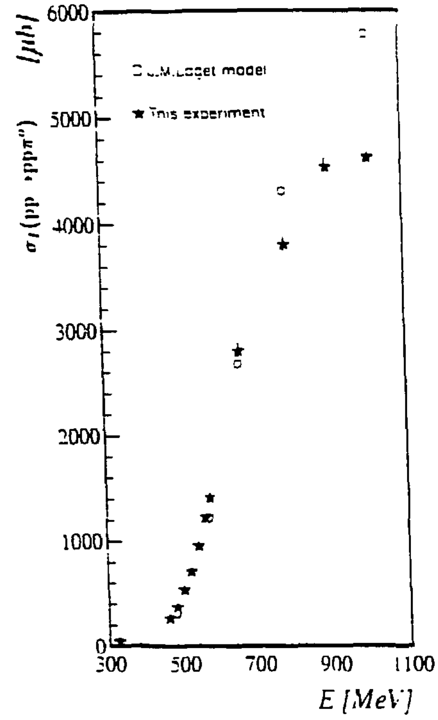

Figure 13

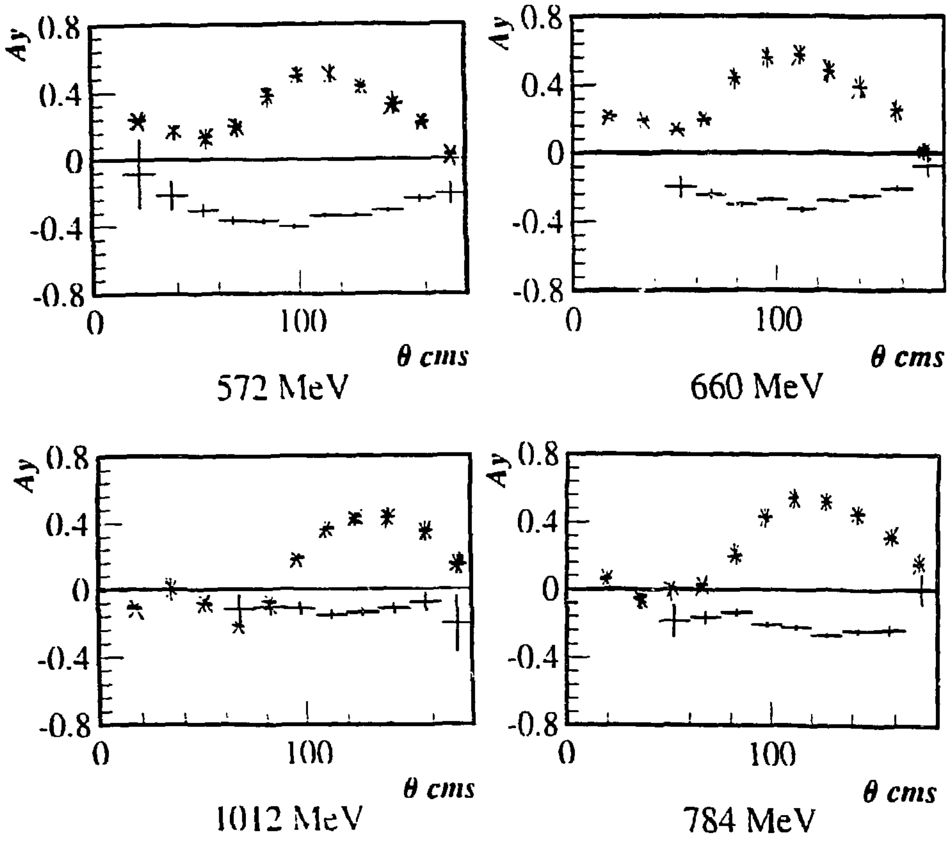

Figure 14

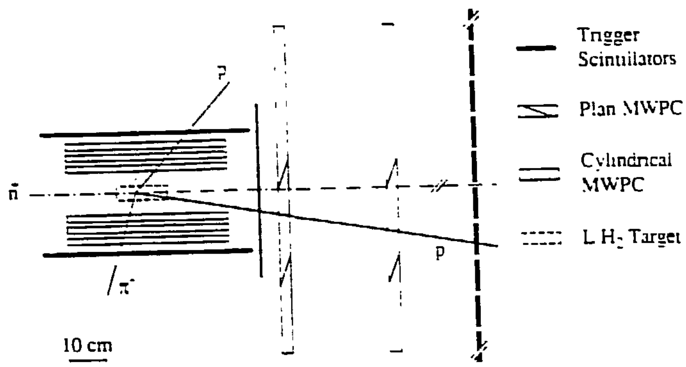

Trigger Scintillators
Plan MWPC
Cylindrical MWPC
L H₂ Target
p
n
π⁻
10 cm

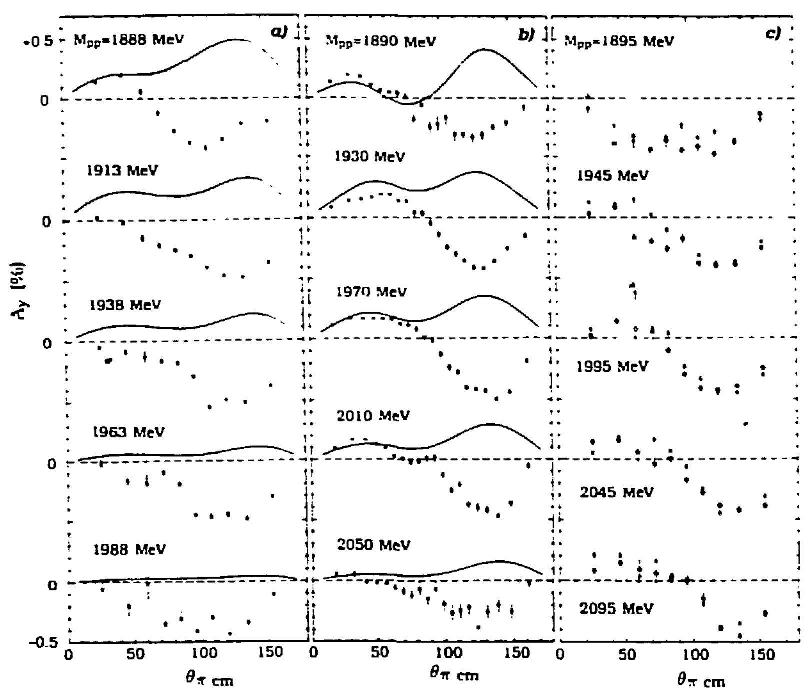

Mpp=1888 MeV
a)
1913 MeV
1938 MeV
1963 MeV
1988 MeV
Mpp=1890 MeV
b)
1930 MeV
1970 MeV
2010 MeV
2050 MeV
Mpp=1895 MeV
c)
1945 MeV
1995 MeV
2045 MeV
2095 MeV
Ay (%)
+0.5
0
-0.5
0
50
100
150
θπ cm

Figure 15

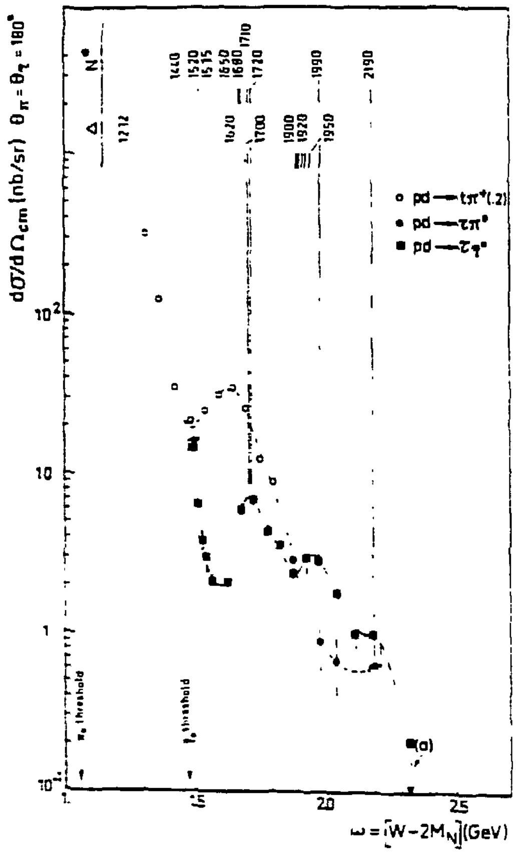

Fig. 16

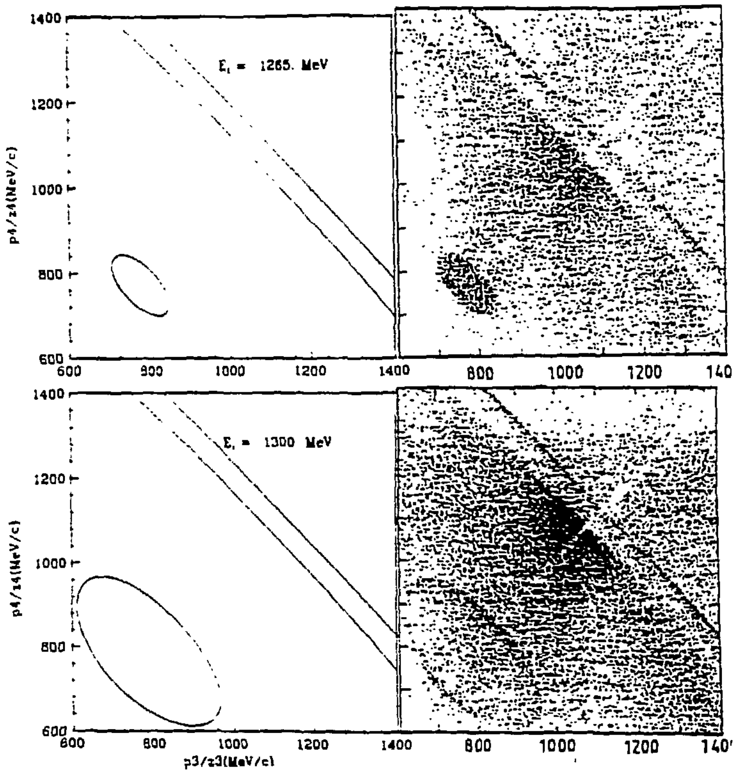

Fig. 17 a. Fig. 17 b.

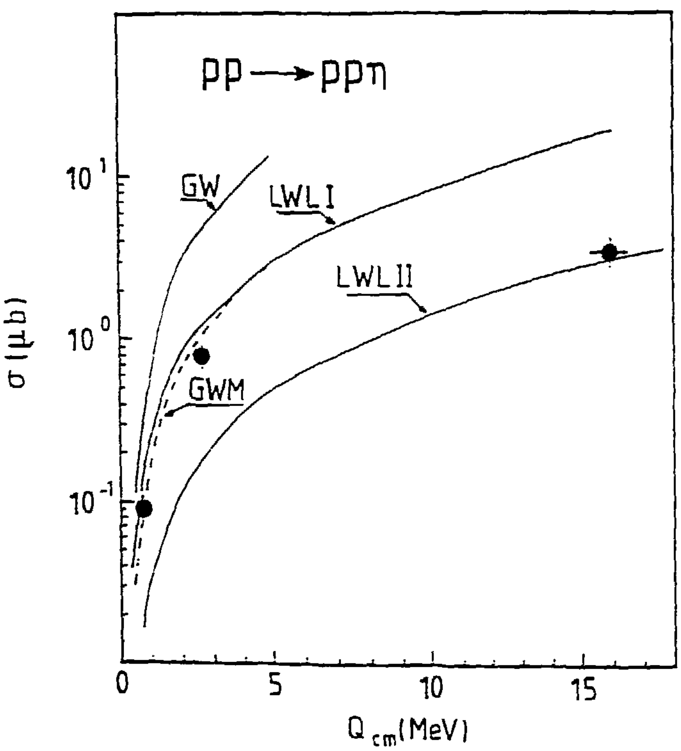

Fig. 18

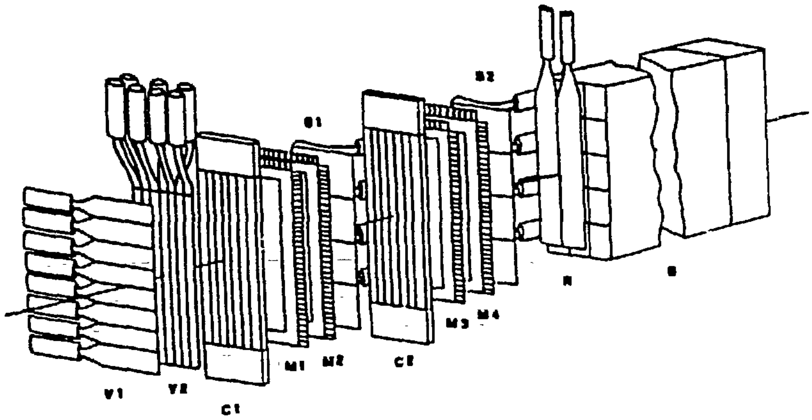

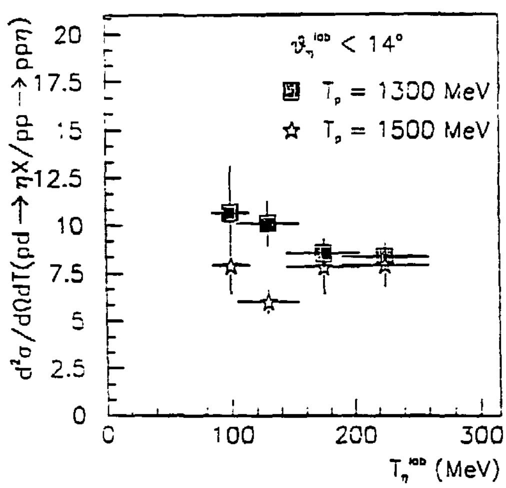
$\vartheta_\eta^{lab} < 14°$
T_p = 1300 MeV
T_p = 1500 MeV
$d^2\sigma/d\Omega dT(pd \to \eta X/pp \to pp\eta)$
0
2.5
5
7.5
10
12.5
15
17.5
20
0
100
200
300
T_η^{lab} (MeV)

Fig. 19

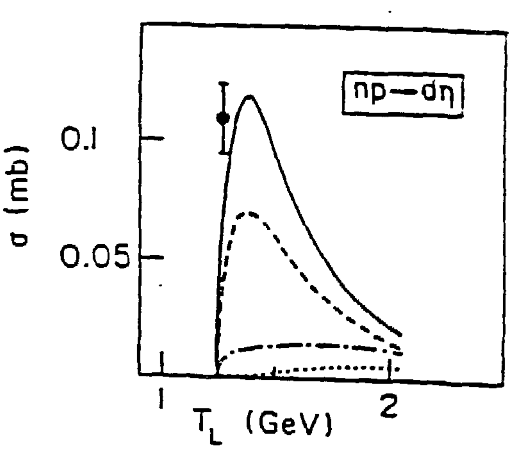
np—dη
σ (mb)
0.1
0.05
1
2
T_L (GeV)

Fig. 20